Tellus (2004), 56A, 79–87

TELLUS

Baroclinic adjustment in the Finnish coastal current

By TAPANI STIPA*, *Finnish Institute of Marine Research, PO Box 33, FIN-00931, Helsinki, Finland*

(Manuscript received 23 January 2003; in final form 19 August 2003)

ABSTRACT

Observations from the northern shore of the Gulf of Finland show a quasi-stable brackish coastal current flowing along a sloping bottom. Other examples of similar currents have been found, for example, in the Arctic basin. Generally, baroclinic flows of this type tend to be unstable. To study the stability of such flows, a specially designed numerical experiment has been devised. The simulations show that a current structure resembling that found in the observations results from an internal baroclinic adjustment of the flow to a baroclinically quasi-stable state with monotonic isopycnal vorticity.

On the basis of the observations and numerical results, we propose that coastal currents for a certain part of the parameter range have an inherent tendency to evolve towards a quasi-stable state. This baroclinic neutralization is suggested as an explanation of the observed persistence of buoyant coastal currents under favorable conditions.

1. Introduction

Persistent, coastally trapped buoyant currents, where isopycnal surfaces as well as the bottom boundary intersect geopotential surfaces, are prominent features on many shelves. They may result from a decreased salinity caused by coastally discharged freshwater, or from diabatic processes. Coastal downwelling and tidal mixing may also in some instances be responsible for the cross-shore buoyancy differences.

There is a wealth of observations indicating the persistence of buoyant coastal currents from around the World; noteworthy examples are the East Greenland Current and the Siberian shelf current. These transport anomalous buoyancy over long distances, and are thus important for teleconnections of water properties. Hence, a knowledge of their stability properties, especially in the Arctic, may be essential for a deeper understanding of the global thermohaline circulation.

Yet no comprehensive theory explaining the persistence of flows of this type has been advanced. Note that a baroclinic flow with constant internal potential vorticity (IPV) in the presence of both a horizontal surface and a horizontal bottom is unstable (Eady, 1949; Charney and Stern, 1962). However, a baroclinic situation where isopycnal and pressure surfaces are not parallel, and the bottom slope is not negligible (i.e. $\frac{\partial h}{\partial y}\frac{N}{f} \approx 1$, where $N^2 = -\frac{g}{\rho}\frac{\partial \rho}{\partial z}$, f is the Coriolis parameter, h is the bottom depth and y is the cross-shore coordinate), is not covered by the usual analytical framework of stability analysis (e.g. Blumsack and Gierasch, 1972). Furthermore, the persistence may result from a non-linear process, as opposed to the linear normal-mode instability found within the most straightforward analytical theories.

Stability inferences from observations are made difficult by the intense tidal mixing taking place over many shelf areas. For example, the Rhine outflow to the North Sea gives a major freshwater signal that would have been very useful in such an analysis. Unfortunately, the density structure of this river plume is substantially modified by tidal stirring (Simpson et al. 1993) and is therefore difficult to interpret in terms of hydrodynamic stability.

The Baltic Sea provides an interesting hydrodynamic laboratory for mixing studies when compared with many other coastal areas. Tides are virtually absent in the Baltic, which favors the development of stable coastally trapped currents. Furthermore, during the spring, double-diffusive processes become negligible (because of the vanishing thermal expansion coefficient, cf. Stipa et al. 1999; Zhurbas and Paka, 1999; Stipa, 2002b) as does the wind stress. The processes that may impair the persistence of coastal currents are thus minimized in the vernal Baltic, and observations can be used with a high level of confidence for making inferences concerning stability.

Using observations from the Baltic as well as numerical experiments, we suggest the possibility that topographically constrained currents might exist because the disintegrating effects of baroclinic instability are inhibited by a sloping bottom under conditions that preclude an analytical resolution of the problem. In Section 2, we present a set of recent observations from the Gulf of Finland, showing the presence of a buoyant coastal current at a considerable distance from the freshwater source. When these observations are compared with already published data for a similar current in the Arctic Ocean (Rudels et al. 2000), it is found that the same parameter regime characterizes both cases.

*Corresponding author
e-mail: tapani.stipa@iki.fi

A numerical experiment described in Section 3 results in a quasi-stable coastal current, which displays a marked similarity with the presently reported field observations. We conclude by comparing our hypothesis with the ideas found in the literature on the baroclinic instability in the presence of a bottom slope as well as sloping isopycnals, and find a little discussed consistency.

2. Observations

2.1. Study area

The Gulf of Finland is an elongated sub-basin of the Baltic Sea (cf. Fig. 1a). It has a length of roughly 400 km and a width varying between 50 and 100 km. The bathymetry is complex, with an irregular and slowly sloping coast on the northern side and a more even, but steeper topography on the southern side. A maximum depth of more than 100 m is found near the southern coast at the entrance from the Baltic proper. A gradual although uneven shoaling takes place towards the east.

The gulf has an open connection to the Baltic Proper, which allows a free water exchange with the open sea. Being in essence an estuary of the Baltic Proper, the haline conditions mainly determine the density stratification in the gulf. The surface salinity varies from roughly 6–7 psu at the entrance to approximately zero in the easternmost end, where the discharge from the largest river debouching into the Baltic, Neva, enters the gulf at St Petersburg (about 60°N, 30°E). A salinity of up to 9–10 psu is found in the near-bottom region of the western gulf.

Already Palmén (1930) showed the existence of a lateral, north–south salinity gradient in the gulf, consistent with the cyclonic circulation he inferred from current observations. After this pioneering study, cross-gulf observations were difficult until the early 1990s. Certain observational progress was made concerning the character of the circulation in the bay from a series of field studies in the early 1990s (Stipa, Tamminen and Seppälä, unpublished; Stipa, 2002b). As a harbinger of studies from the era of increased international co-operation, a thorough review of the available literature on the physical conditions of the gulf has recently been given by Alenius et al. (1998).

An important parameter for the dynamic regime of the gulf is the ratio of its width to the baroclinic Rossby radius, $1 < L/L_{Ro} \leq 10$ (typical values for the Rossby radius in the Baltic are ∼2–5 km, Fennel et al. 1991a). On the other hand, the baroclinic forcing from the Neva is strong (the annual mean discharge is about 2500 $m^3\ s^{-1}$, cf. Bergström & Carlsson, 1994). Both factors in combination lead us to expect baroclinic instability to be a major process affecting the circulation in the Gulf, at least during the spring season when the wind stress is rendered negligible by a stable atmospheric boundary layer, cf. Fig. 1b.

A further important aspect is the Lagrangian advective timescale associated with the Neva outflow, which (assuming a steady westward flow of ∼0.1 $m\ s^{-1}$) can be estimated as about 1 month. Hence, a coastal current is expected to establish itself along the northern coast in a relatively short time even after a violent storm. If such a current is stable, it could exert a considerable influence on the transport of the largely untreated waste waters from St Petersburg (Pitkänen and Tamminen, 1995).

Furthermore, the bathymetry only has a mean slope of roughly 10^{-3} adjacent to the northern coast, whereas in the southern part of the gulf it is fairly steep. Since the intersection of density surfaces with a sloping bottom is known to significantly influence the properties of free boundary waves (Rhines, 1970) as well as the non-linear circulation (Rhines, 1977; Hallberg and Rhines, 1996, 2000), significant topographic influence on the flow is expected.

2.2. Description of observations

Observations from the entrance to the Gulf of Finland will be used to illuminate the persistence and time dependence of a buoyant coastal current when the disturbing effects, in particular the wind stress, are at a minimum. Our data consist of eight snapshots of a single south–north transect (Fig. 1) obtained between April 21 and June 16, 1993. The observation platform was a rented 15 m oak trawler (M/S Jette), which was equipped with a differential GPS and a manually deployed SiS CTDPlus 100 sonde. The CTD accuracy was checked against water samples with a salinometer (AutoSal) and found to be within 0.03 psu, which is as good a field calibration as can be obtained in the Baltic due to the strong salinity gradients here compared with the ocean.

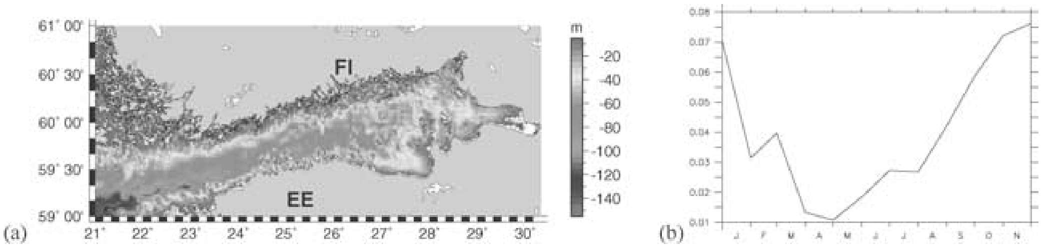

Fig 1. (a) Gulf of Finland with bathymetry according to Seifert and Kayser (1995); (b) mean monthly wind stress (N m^{-2}) from NCEP/NCAR analysis above the northern Baltic Sea (59°N, 20°E).

The vertical density distribution over the transects are shown in Fig. 2. For later reference the inverse bottom profile is included in the graphs.

A buoyant, baroclinic coastal current, caused by a salinity anomaly (cf. Stipa, 2002b) is seen in Figs. 2a–f , i.e. from April 21 to May 27, coinciding with the climatological wind-stress minimum period. A moderate storm occured at the end of May, which resulted in the disappearance of the current (Figs. 2g and h). During the observation period, the surface density in the core of the current decreased slightly, due to a gradual warming and freshening of the surface layer.

The slope of the bottom in the measurement area of Fig. 2 is very variable over small scales, as recognized from the small displacements (of the order of 100 m) between the transects. However, a mean slope of approximately 0.003 may be estimated. It is interesting to note that for the sections where the coastal current manifests itself in the form of tilted isopycnals, the slope of the bottom profile is not too different from that of the density surfaces. This feature of the current will be elaborated on in Section 3.

The transport of freshwater associated with the hydrographic cross-sections of Fig. 2 can be estimated from the area of the jet (7 km by 20 m), the mean velocity in the core (of the order of 0.2 m s^{-1}, from Acoustic Doppler Current Profiler (ADCP) measurements (not shown)) and a salinity anomaly of 0.7 psu. The result is approximately 3000 m^3 s^{-1}, which is close to the total freshwater discharge into the Gulf of Finland.[1]

This current can be inferred to exist in the absence of external forcing, i.e. as a result of processes internal to the sea. The wind stress during the observation season is small, as discussed. The influence of the freshwater forcing from Neva, on the other hand, can be decomposed into two factors: the barotropic effect (addition of mass) and the baroclinic effect (creation of a salinity anomaly). The barotropic adjustment takes place on scales of the order of the barotropic Rossby radius, which is hundreds of kilometers for the Gulf of Finland; in essence, the barotropic adjustment is expected to actively modify processes on a very large-scale compared with the width of the current in Fig. 2. The immediate baroclinic forcing, on the other hand, is limited to a length scale of the local baroclinic deformation radius, a few kilometers at the river entrance. The momentum input from the Neva has a direct range corresponding to the local inertial radius $Uf^{-1} \approx 10$ km. Although these scales are not truly separable in the presence of a sloping bottom, we may infer that the Neva can hardly exert a driving force on the observed current, other than via the creation of a low-salinity water mass.

Indeed, a similar current has been documented by Rudels et al. (2000) in the Arctic Ocean, another area where tidal mixing and other external forcing is weak. In their observations, the bottom slope of ≈ 0.03 is larger by an order of magnitude than in the Gulf of Finland, but the stratification is an order of magnitude weaker ($Nf^{-1} \approx 10$), so that $(\partial h/\partial y)\, Nf^{-1}$ is approximately the same as that characterizing the observations shown in Fig. 2.

[1] A similar calculation was first made by J. Rodhe (*pers. commun.*, 1981) during a course of the Nordic Oceanographic Collegium several years earlier.

2.3. A discrepancy between the observations and the theory

A flow with linearly sloping isopycnals, intersecting both the bottom and the surface, is baroclinically unstable in the quasi-geostrophic solution to the Eady problem, even with the bottom inclination included in the analysis (Blumsack and Gierasch 1972; Stipa, 2002a). As shown in Fig. 3, the growth rate of the instability is significantly modified by the bottom slope for the type of flow depicted in Fig. 2 ($\Delta < 0$). In particular the long waves (small non-dimensional wavenumbers r_h) are already stabilized for small bottom slopes.

However, at the short-wave end of the spectrum an unstable regime remains that would have sufficient growth rates to render the coastal current unstable over an advective timescale defined on the basis of the distance between the observation site and the freshwater source. The maximum growth rate for the situation depicted in Fig. 2 ($\Delta \approx -1$) is still about 50% of the growth rate for the flat-bottom case (of the order of 10 days).

With $(\partial h/\partial y)\, Nf^{-1} \approx 0.3 < 1$ in Fig. 2, the quasigeostrophic boundary wave dispersion relationship is still relevant (Rhines, 1970; Huthnance, 1978), but a Kelvin-type balance also starts to play a role for the dynamics. Clearly, there is a discrepancy between the quasigeostrophic theory and the observations and it has been judged that numerical experiments may provide deeper understanding of the processes governing a flow of the type seen in the observations.

3. Numerical experiments

The existence of instabilities in initial-value experiments for a system resembling the Gulf of Finland has been documented by Stipa (1999). These experiments showed that while instabilities exist in a coastal current, they can be arrested by bottom topography. However, the process of arresting is very sensitive to the chosen initial conditions, apparently because no simple analytical condition or prescribed potential vorticity distribution can describe the balance in this type of flow. The experiments also showed that the model does produce vigorous baroclinic instabilities under most circumstances.

Therefore, in order to investigate the quasi-stable state of a coastal flow of the type shown in Fig. 2, we have performed additional numerical experiments with a non-linear three-dimensional Boussinesq solver (Marshall et al., 1997a,b). Rather than specifying a suitable initial condition from analytical results, the experimental strategy is: (1) to initialize the stratification by forcing the model with a boundary condition for a certain

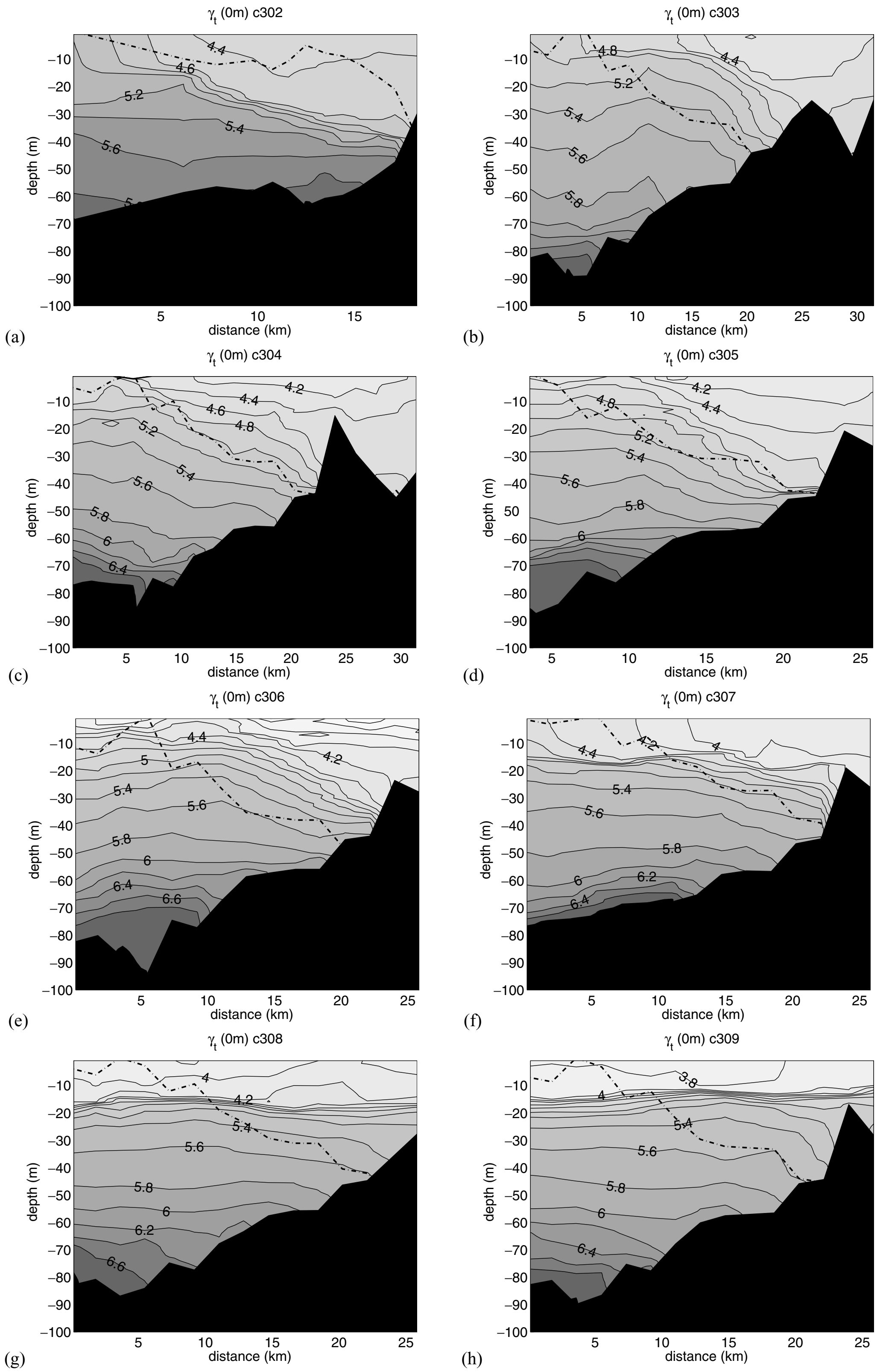

Fig 2. A south–north section (59°28–59°45N, along 22°55E) of measured density structure at the entrance to the Gulf of Finland in April–July, 1993. The dash-dotted line represents the bottom profile reflected across the horizontal. The dates for the transects were: 21 Apr (c302), 29 Apr (c303), 5 May (c304), 12 May (c305), 19 May (c306), 27 May (c307), 10 May (c308), 16 May (c309)

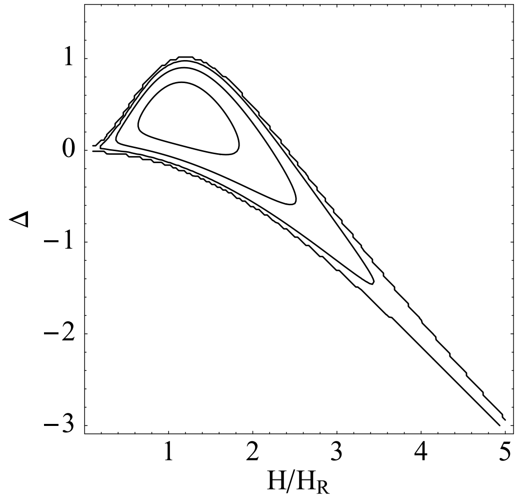

Fig 3. Non-dimensional growth rate $\sim\omega_+$ as a function of the non-dimensional wavenumber (expressed as the ratio of domain height to the Rossby height $r_h \equiv H H_R^{-1} = \frac{Hf}{kN}$) and the ratio of bottom slope to isopycnal slope $\Delta = \frac{\partial h}{\partial y}\sigma^{-1}$. Contours 0, 0.1, 0.2 and 0.3 are drawn. The orientation of the density field structures in Fig. 2 correspond to $\Delta \approx -1$. $\Delta = 0$ is the traditional Eady problem. Constructed on the basis of Blumsack and Gierasch (1972) and Stipa (2002a).

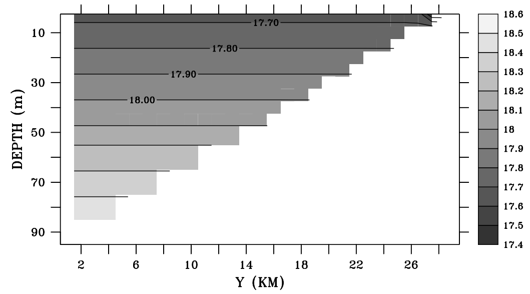

Fig 4. Model channel side view with the initial density stratification ($\gamma = \rho - 1000$ kg m^{-3}). The channel is 100 km long and periodic in the east–west (x) direction, cf. Fig. 5.

period; (2) to terminate the forcing; and (3) to allow the model to adjust to a stable state through its internal dynamics. The term stable in the present numerical context refers to a vanishing time evolution of the mean cross-channel density structure, which is not strictly identical to the analytical concept of no growing infinitesimal perturbations.

The model geometry is a channel, periodic in the east–west direction with a vertical wall in the south and a sloping bottom reaching the surface at the northern boundary (Fig. 4). Motivated by the observations presented in Section 2, the channel is taken to have a width of 30 km, a length of 100 km and a depth of 100 m in the south. The spatial discretization is 1 km in the horizontal and 5–10 m in the vertical. Horizontal subgrid-scale eddy diffusion is modeled using a biharmonic operator, with $k_{h4} = 8 \times 10^6$ m^4 s^{-1} for momentum and $k_{h4} = 2 \times 10^6$ m^4 s^{-1} for tracers. The vertical diffusion was specified following Pacanowski and Philander (1981), with minimum and maximum diffusivity as 10^{-6} and 10^{-3} m^2 s^{-1}, respectively. A quadratic bottom stress with $C_d = 10^{-3}$ was used during the forcing stage of the experiment. For this choice of parameters, a time-step of 300 s was found to be appropriate.

The initial condition used in the model integration is a quiescent and horizontally homogeneous state. The motion is set up by a prescribed freshwater forcing, numerically simulated by smoothly removing salt at the northern boundary from the initially stratified water column ($N = 10^{-2}$ s^{-1}, cf. Fig. 4). The potential density anomaly is a linear function of salinity, $\gamma = \rho_0 (1 + \beta s) - 1000$ kg m^{-3}. The salt forcing, $\rho \frac{\partial s}{\partial t} = s \nabla \cdot \boldsymbol{J}_m$, is taken to be stochastic with a white-noise spectrum both in frequency and along-channel wavelength, with $\boldsymbol{J}_m = -10^{-2}\,[0.5 + U(1)]$ kg m^{-2} s^{-1} $\boldsymbol{k}$ for the two northernmost grid cells ($U(1)$ is the uniform random distribution of unit width). The randomness acts as an initial disturbance for possible amplifying motions (cf. Jones and Marshall 1997). Since s in forced cells decreases quickly towards zero, so does the amplitude of the disturbances.

The time evolution of the surface-layer density field is shown in Fig. 5. The initial development of the current structure is characterized by a rapid decrease of salinity at the northern boundary to values close to zero. Subsequently, the developing cross-shore density gradient becomes stronger and spreads towards the interior by eddy fluxes resulting from baroclinic instability. The eddies are initially small because of the small depth, but soon increase in size as the buoyancy structure spreads by mixing to deeper water.

The forcing was terminated after 100 days, when a strong, baroclinic coastal current has developed. During the subsequent non-forced integration of 50 days, the model finds its way to the marginally stable, baroclinically neutral state by adjusting the unstable stratification through baroclinic instability in small steps (cf. Stone, 1978; Lindzen, 1993). The adjusted result after 150 days is shown in Fig. 6. Some long-lived eddies, which arose during the adjustment process, are seen on the southern side of the channel, but the flow on the northern side has assumed a steady geostrophic character with no growing disturbances. The eddies grow until they fill the domain outside the coastal jet, as expected based on the results due to Rhines (1977).

The velocity field of a cross-section in the adjusted state, shown in Fig. 6a, has a strong westward jet along the northern coast. This jet is associated with a density structure (Fig. 6b) where the isopycnals are almost horizontal in the southern part of the channel, but turn towards the bottom in the jet region. There is a very interesting resemblance between the adjusted density structure in the model and that seen in the observations, particularly in Figs. 2b–e. Additionally, Fig. 7 shows the eddy momentum flux, defined as the correlation of deviations from the along-channel mean, $-\rho\overline{u'v'}\boldsymbol{e}_y - \rho\overline{u'w'}\boldsymbol{e}_z$, and its divergence for day 150.

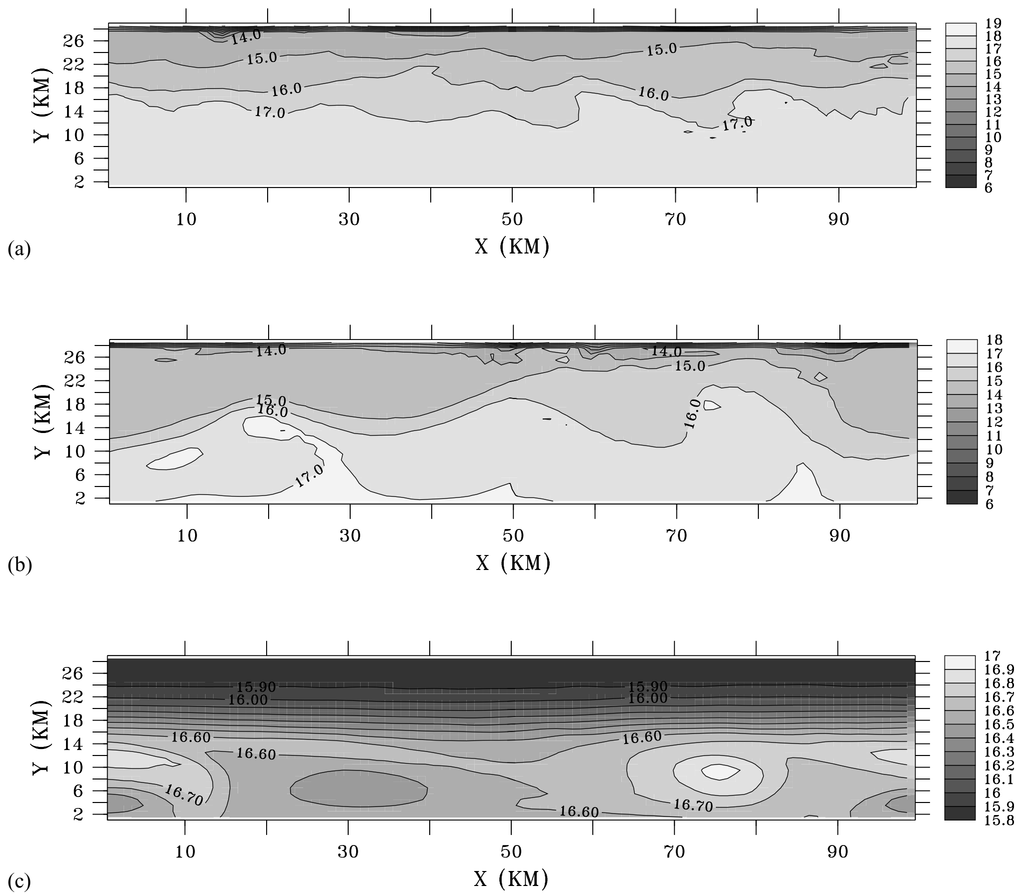

Fig 5. Process of baroclinic adjustment as seen by surface densities, (a) after 50 and (b) 100 days of salt removal (c) after an additional 50 days with no forcing at all.

4. Discussion and conclusions

Field observations, as summarized in Section 2, show the presence of a persistent, coastally trapped current along the northern coast of the Gulf of Finland when disturbing effects are at a minimum. This current is much more sharply defined in the present set of observations than in the coarser fields examined by (Palmén, 1930). The sharp boundaries of the current suggest that the water masses retain their properties during their progression along the coast. The nature of the current, as well as its freshwater transport, suggest the river Neva as its largest contributor. Hence, the parts of the Neva-borne effluents that are not sedimented are transported rapidly along the Finnish coast.

The baroclinic stability of a current, where the density surfaces as well as the bottom towards which these are inclined have large and comparable slopes, has not been comprehensively discussed in the literature. The quasigeostrophic Eady problem in the presence of an infinitesimal bottom slope has been considered by, for example, Blumsack and Gierasch (1972). They show that perturbations of small wavenumber are considerably stabilized compared with the situation without a bottom slope, but a narrow unstable range at large wavenumber remains for all values of the slope, cf. Fig. 3. Friction in the form of Ekman pumping is found to destabilize the flow for all wavenumbers (Williams and Robinson, 1974; Stipa, 2002a). Lateral friction in the numerical model was observed not to be sufficient to suppress the instability altogether in the present experiment, and no stabilization was observed for experiments with a flat bottom.

Therefore, stability of the type seen in the observations and numerical results cannot be explained on the basis of the quasigeostrophic theory. It can be suggested that the unstable region of the quasigeostrophic solution might be stabilized by small changes in the propagation characteristics of the edge wave along the sloping bottom, possibly due to non-quasi-geostrophic effects, or if the perturbations become arrested by the self-advection of their PV fields (Bell, 1992).

On the other hand, Lindzen (1994) introduced slight modifications of the constant shear in the Eady problem, and found a substantial stabilization of in particular long waves, apparently related to the propagation characteristics of edge waves. Hence,

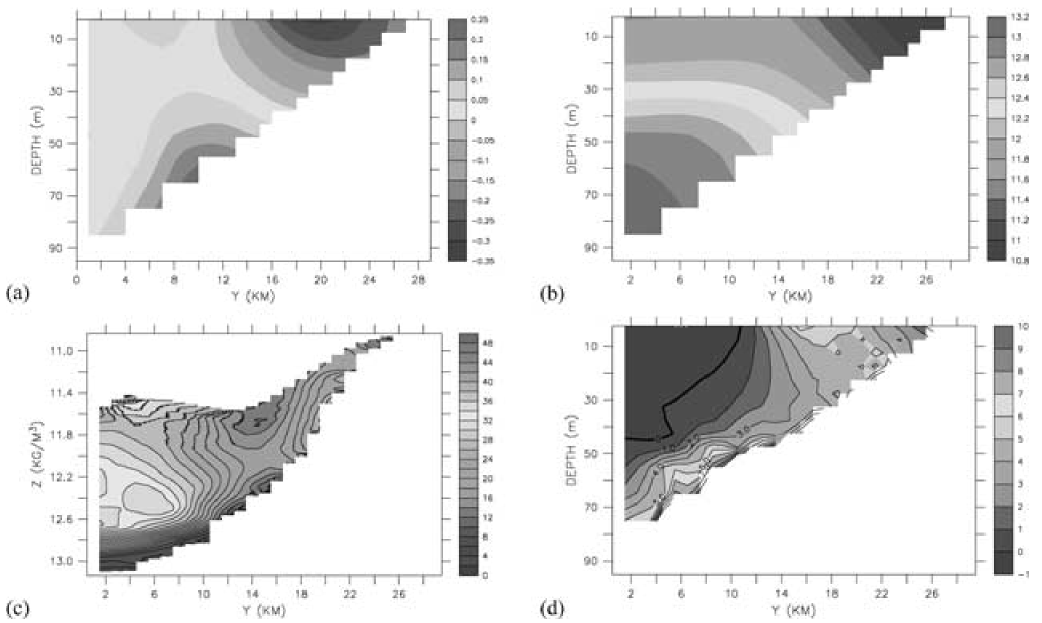

Fig 6. Baroclinically adjusted state as an along-channel mean on day 150 (a) in velocity field and (b) the density field and (c) isopycnal hydrostatic PV field $[(f + (\nabla \times \boldsymbol{v}) \cdot \boldsymbol{k}]\frac{\partial \rho}{\partial z})$, in 10^{-8} m s (d) along-channel mean of isopycnal slope $((\partial \rho/\partial z)^{-1} \partial \rho/\partial y)$.

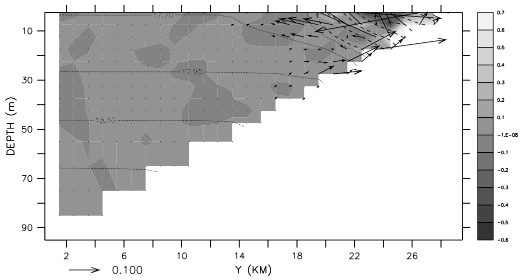

Fig 7. Wave radiation stress flux (arrows), its divergence (shading, scaled with 10^3), and density (γ, contours) on day 150.

a shear structure that deviates from that associated with the traditional Eady problem may also be an important factor for the stabilization.

The numerical experiment described in Section 3 supports this stabilization hypothesis. During a gradual spin-up of the coastal buoyancy anomaly, the flow adjusts itself through internal dynamics to a balanced, quasi-stable state. In this state, the flow persists over protracted periods. This process is reminiscent of the baroclinic adjustment in the atmosphere as proposed by Stone (1978).

The isopycnal potential vorticity field (Fig. 6c) shows that local IPV extrema in the jet region have disappeared and the isopycnal gradient of PV is definite in sign. However, the IPV is not entirely homogeneous in the southern part of the channel due to the eddy activity seen in Fig. 5c. As Fig. 6d shows, the isopycnal slope of the baroclinic area near the coast in the adjusted state is within a factor of 3 of that characterizing the bottom contour of slope 0.003. On the other hand, this also means that the Rossby number $Ro = |\sigma| N f^{-1}$ (where σ is the isopycnal slope) is of the order of 1.

Hence, as in the Eady problem, the internal distribution of potential vorticity in the jet region of the model does not show clear extrema in the baroclinically adjusted state. Since a local extremum of PV satisfies the necessary condition for baroclinic instability (Charney and Stern, 1962) and is therefore effectively removed, the PV distribution in the model is consistent with quasigeostrophic stability theorems. What is currently not well understood and deserves a further study is the question of the inefficiency of the Eady instability mechanism for edge wave interaction, where the wave stress radiation may have an influence. The wave stresses in Fig. 7 act to decelerate the bottom flow and to accelerate the surface flow at the front.

Other theories explaining the persistence of the coastal currents have been advanced. The Ekman transport in the bottom boundary layer, which makes the bottom "slippery" for the flow, is frequently discussed in combination with shelf fronts. For instance, Chapman and Lentz (1994, 1997) presented model results illustrating the offshore movement of a shelf front by a bottom boundary layer. However, the exclusion of non-linear momentum advection terms in that model does not necessarily do justice to the baroclinic adjustment process demonstrated in the present study in the absence of bottom friction.

It is nevertheless clear that the bottom boundary layer plays a role under some circumstances, perhaps not in the trapping of coastal buoyancy anomalies, but certainly for modifying their properties and by also creating other instabilities (such as the symmetric instability in the bottom boundary layer as discussed by Allen and Newberger, 1998).

In the barotropic arrested topographic wave model due to Csanady (1978), bottom friction will lead to an eventual spreading of the flow. This is, however, strictly only true for the barotropic case; in a baroclinic situation such as the one studied here, PV moves solely along isopycnals (Haynes and McIntyre, 1987) and no spreading occurs. Only a change in density, such as resulting from mixing, for example, can induce a widening of isopycnal surfaces and hence a spreading of the current. However, the stability problem can be expected to be modified by a boundary source of vorticity, as found in the quasigeostrophic solution with Ekman pumping.

The present study has argued in favour of an alternative explanation for the existence of persistent buoyant currents at coastal margins: baroclinic instability, which on general grounds is expected to lead to disintegration of the flow, in fact acts to bring the flow to a baroclinically quasi-stable state.

5. Acknowledgments

The author has been consistently funded by the Maj and Tor Nessling foundation. The numerical solutions are a consequence of inspiration from co-operation with J. Marshall (MIT). Discussions with P. Lundberg and J. Nilsson at Stockholm University greatly helped in the final shaping of the article. T. Tamminen arranged the funding for the measurements, shared the field work and together with J. Seppālā was instrumental in the success of the expeditions. The scientific equipment and logistics were provided by Tvärminne Zoological Station. Our captains Sture Berndtson and Epa Tamminen are also gratefully acknowledged. NCEP Reanalysis data were provided by the NOAA-CIRES Climate Diagnostics Center, Boulder, CO, USA, from their Web site at http://www.cdc.noaa.gov/.

References

Alenius, P., Myrberg, K. and Nekrasov, A. 1998. The physical oceanography of the Gulf of Finland: a review. *Boreal Environ. Res.* **3**(2), 97–125.

Alenius, P., Nekrasov, A., Myrberg, K. 2003. Variability of the baroclinic Rossby radius in the Gulf of Finland. *Cont. Shelf Res.* **23**, 563–573.

Allen, J. S. and Newberger, P. A. 1998. On symmetric instabilities in oceanic bottom boundary layers. *J. Phys. Ocean.* **28**, 1131–1151.

Bell, M. J. 1992. The nonlinear evolution of a slowly growing wave on a laterally sheared baroclinic flow. *J. Fluid Mechan.* **241**, 615–643.

Bergström, S. and Carlsson, B. 1994. River runoff to the Baltic Sea: 1950–1990. *Ambio* **23**(4–5), 280–287.

Blumsack, S. L. and Gierasch, P. J. 1972. Mars: the effects of topography on baroclinic instability. *J. Atmos. Sci.* **29**, 1081–1089.

Chapman, D. C. and Lentz, S. J. 1994. Trapping of a coastal density front by the bottom boundary layer. *J. Phys. Ocean.* **24**(7), 1464–1479.

Chapman, D. C. and Lentz, S. J. 1997. Adjustment of stratified flow over a sloping bottom. *J. Phys. Ocean.* **27**, 340–356.

Charney, J. G. and Stern, M. E. 1962. On the stability of internal baroclinic jets in a rotating atmosphere. *J. Atmos. Sci.* **19**, 159–172.

Csanady, G. T. 1978. The arrested topographic wave. *J. Phys. Ocea.* **8**, 47–62.

Eady, E. T. 1949. Long waves and cyclone waves. *Tellus* **1**(3), 33–52.

Fennel, W., Seifert, T. and Kayser, B. 1991. Rossby radii and phase speeds in the Baltic Sea. *Cont. Shelf Res.* **11**, 23–36.

Hallberg, R. and Rhines, P. 1996. Buoyancy-driven circulation in an ocean basin with isopycnals intersecting the sloping boundary. *J. Phys. Ocean.* **26**, 913–940.

Hallberg, R. and Rhines, P. 2000. Boundary sources of potential vorticity in geophysical applications. In: *Developments in Geophysical Turbulence Fluid Mechanics and its Applications,* vol. 58, eds.R. M. Kerr and Y. Kimura). Kluwer, Dordrecht.

Haynes, P. H. and McIntyre, M. E. 1987. On the evolution of vorticity and potential vorticity in the presence of diabatic heating and frictional and other forces. *J. Atmos. Sci.* **44**(5), 828–841.

Huthnance, J. M. 1978. On coastal trapped waves: analysis and numerical calculation by inverse iteration. *J. Phys. Ocean.* **8**, 74–92.

Jones, H. and Marshall, J. 1997. Restratification after deep convection. *J. Phys. Oceanogr.* **27**, 2276–2287.

Lindzen, R. S. 1993. Baroclinic neutrality and the tropopause. *J. Atmos. Sci.* **50**(8), 1148–1151.

Lindzen, R. S. 1994. The Eady problem for a basic state with zero PV gradient but $\beta \neq 0$. *J. Atmos. Sci.* **51**(22), 3221–3226.

Marshall, J., Adcroft, A., Hill, C., Perelman, L. and Heisey, C. 1997a. A finite-volume, incompressible Navier Stokes model for studies of the ocean on parallel computers. *J. Geophys. Res.* **102**(C3), 5753–5766.

Marshall, J., Hill, C., Perelman, L. and Adcroft, A. 1997b. Hydrostatic, quasi-hydrostatic, and non-hydrostatic ocean modeling.. *J. Geophys. Res.* **102**(C3), 5733–5752.

Pacanowski, R. C. and Philander, S. G. H. 1981. Parameterization of vertical mixing in numerical models of tropical oceans. *J. Phys. Ocean.* **11**, 1443–1451.

Palmèn, E. 1930. Untersuchungen über die Strömmungen in den Finnland umgebenden Meeren. *Commentationes Physico-Mathematicae* **12**, 45–94. Studies on the currents in the seas surrounding Finland (in German).

Pitkänen, H. and Tamminen, T. 1995. Nitrogen and phosphorus as production limiting factors in the estuarine waters of the eastern Gulf of Finland. *Marine Ecol. Progr. Series* **129**, 283–294.

Rhines, P. 1970. Edge-, bottom-, and Rossby waves in a rotating stratified fluid. *Geophys. Fluid Dyn.* **1**, 273–302.

Rhines, P. 1977. The dynamics of unsteady currents. In: *The Sea,* vol. VI, Wiley, New York, 189–318.

Rudels, B., Muench, R. D., Gunn, J., Schauer, U. and Friedrich, H. J. 2000. Evolution of the Arctic Ocean boundary current north of the Siberian shelves. *J. Marine Syst.* **25**, 77–99.

Seifert, T. and Kayser, B. 1995. A high resolution spherical grid topography of the Baltic Sea. *Meereswissenschaftliche Berichte* **9**, 72–88. (Summary in German and English.)

Simpson, J. H., Bos, W. G., Schirmer, F., Souza, A. J., Rippeth, T. P., Jones, S. E. and Hydes, D. 1993. Periodic stratification in the Rhine ROFI in the North Sea. *Oceanologica Acta* **16**(1), 23–32.

Stipa, T. 1999. Instabilities and along-shore variability in the Finnish coastal current. In: *4th Workshop on Physical Processes in Natural Waters,* 13–17 September 1999, Roosta, Estonia, Report series, vol. 10, Estonian Marine Institute, Tallinn, 62–66.

Stipa, T. 2002a. *Freshwater, Density Gradients and Biological Processes in Cold, Brackish Seas: Aspects of the Biogeophysical Fluid Dynamics Characterising the Baltic Sea*. PhD Thesis. Department of Meteorology, Stockholm University.

Stipa, T., 2002b. Temperature as a passive isopycnal tracer in cold, spiceless oceans. *Geophys. Res. Lett.* **29**(20), 10.1029/2001GL014532.

Stipa, T., Tamminen, T. and Seppälä, J. 1999. On the creation and maintenance of stratification in the Gulf of Riga. *J. Marine Syst.* **23**, 27–49.

Stone, P. 1978. Baroclinic adjustment. *J. Atmos. Sci.* **35**, 561–571.

Williams, G. P. and Robinson, J. B. 1974. Generalized Eady waves with Ekman pumping. *J. Atmos. Sci.* **31**, 1768–1776.

Zhurbas, V. M. and Paka, V. T. 1999. What drives thermohaline intrusions in the Baltic Sea? *J. Marine Syst.* **21**, 229–241.